

# Morphological Clustering Filter for Wavelet Shrinkage Improvement

Jinsung Oh, Heesoo Hwang, Changhoon Lee, and Younam Kim

**Abstract:** To classify the significant wavelet coefficients into edge area and noise area, a morphological clustering filter applied to wavelet shrinkage is introduced. New methods for wavelet shrinkage using morphological clustering filter are used in noise removal, and the performance is evaluated under various noise conditions.

**Keywords:** Morphological filter, wavelet shrinkage, noise reduction.

## 1. INTRODUCTION

The common method for de-noising in the wavelet domain is to compute the wavelet decomposition of the noisy signal and then to manipulate the wavelet coefficients at each level. The manipulation can be done using hard or soft thresholding methods, called wavelet shrinkage [1-4], in which the significant wavelet coefficients that are supposed to be affected by noise are replaced by zero or another suitable value. Since the wavelet transform allows exceptional localization in both the time and frequency domains, the selective filtering techniques using edge information obtained by the correlation technique [5], the probability density function [6] or zero-crossing [7] can improve the de-noising performance. The de-noising performance depends on finding the location of edges, i.e., separation of significant wavelet coefficients due to edges from wavelet coefficients as result of noise. To classify the significant wavelet coefficients into edge area and noise area, this paper proposes a morphological clustering filter that can be applied to wavelet shrinkage.

## 2. GEOMETRICAL INTERPRETATION OF WAVELET COEFFICIENTS

Fig. 1 shows the two-dimensional wavelet transform representation of the “House” image using Daubechies wavelet  $D_3$  [8]. As shown in Fig. 1, a coherent edge appearance in the different wavelet domain is observed and the high bands seem to reveal the edge characteristics. As pointed out in [9,10], however, the high bands are mostly speckled or have speckle-like edges with the loss of structured geometry, which means the geometrical filtering techniques on the high bands, for instance, the median filter, are

inappropriate since speckled components are removed by the nonlinear filtering technique. Fig. 1 shows the location of significant coefficients with respect to an absolute threshold of 20 in the wavelet domain for the “House” image. As one can see, spatial clustering of significant coefficients in the high bands is observed. Therefore, it is suggested that a morphology-based nonlinear partitioning of the wavelet coefficients into edge area and non-edge area can be applied since the non-clustering area can be easily suppressed by the use of binary mathematical morphology. The first attempt using morphology for the application of image compression has been proposed in [11]. In [11], the regions having significant coefficients (indicating the presence of edges) are obtained by hard thresholding and then dilation operation is applied. Using dilation, the area of the single significant coefficient is enlarged to include neighborhoods, which can alleviate the distortion of edges for reconstruction of the compressed image. However, this simple dilation operation is not useful when the input image is corrupted by noise. In the case of a noisy image, we need to develop a sophisticated morphological operator that can preserve the significant coefficients of the edges with the removal of the significant coefficient due to the noise.

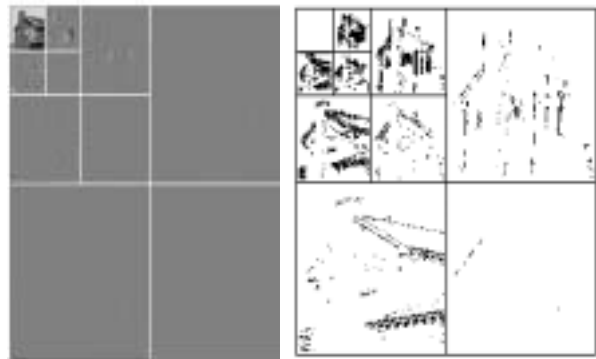


Fig. 1. 2-D wavelet transform of the “House” image and its location of significant coefficients.

Manuscript received May 28, 2002; accepted September 25, 2002.

J. Oh, H. Hwang, C. Lee and Y. Kim are with the School of Electrical Engineering., Halla University, San 66, Heungup, Wonju, Kangwon, 220-712, Korea (e-mail: jsoh@hit.halla.ac.kr).

### 3. MORPHOLOGICAL CLUSTERING FILTER

The multiresolution support [3] indicates where the significant wavelet coefficients are and permit the recognition of all information concerning the given images (edge, noise, etc.). The multiresolution support can be easily obtained by thresholding the wavelet coefficients. The multiresolution support at the level  $l$ , denoted as  $S^l$ , is given by

$$S^l(\underline{n}) = \begin{cases} 1, & |w_l(\underline{n})| > T \\ 0, & |w_l(\underline{n})| \leq T \end{cases} \quad (1)$$

where  $\underline{n}$  denotes two-dimensional variables,  $w_l(\underline{n})$  is the wavelet coefficients at level  $l$ , and  $T$  is the threshold value. Fig. 2 show a two-dimensional wavelet transform representation of a noisy "House" image corrupted by zero-mean Gaussian noise with a variance of  $\sigma_n^2$  and its multiresolution support where  $T$  is  $2\sigma_n$ . As can be seen, the location of significant coefficients by the edges remains with the spatial clustering. However, the location of the significant coefficients due to the noise is also detected but randomly distributed. Clearly, the multiresolution support representation has the geometrical information of significant coefficients by the edges, which indicates that geometrical filtering techniques using binary mathematical morphology can be applied to the multiresolution support.

The definition of morphological clustering filter (MCF) applied on the multiresolution support  $S^l$  is as follows:

$$\left\{ \max_{i \in \{1, \dots, M\}} \left[ (S^l \ominus B_i)(\underline{n}) \right] \right\} \oplus B_F(\underline{n}), \quad (2)$$

where  $B_i$  is a flat structuring element in one of four possible directions and  $B_F$  is the union of the  $B_i$ s (see Fig. 3). Specifically, the morphological clustering filter has a maximum of directional erosions ( $\ominus$ ) followed by dilation ( $\oplus$ ) with the flat structuring element. The directional erosion can remove isolated noises, but preserve directional patterns. And the dilation operation can widen directional area output filtered by erosion. It is shown that these directional morphological filtering techniques [12] remove the noise effectively while preserving detail of the edges.

Using 4 directional structuring elements each with a size of  $1 \times 3$ , the morphological clustering filtered output applied on  $S^{LH^2}(\underline{n})$  is shown in Fig. 4. As can be seen in Fig. 4, the morphological clustering filter removes the location of the significant coefficients

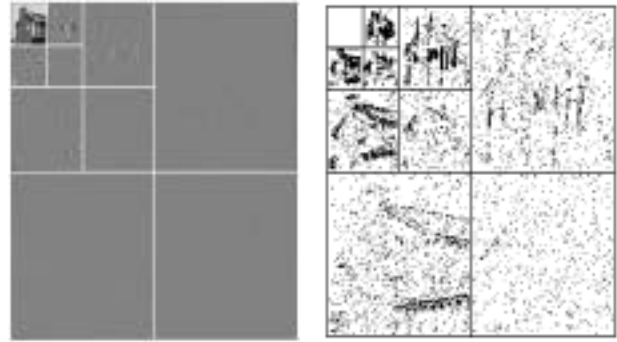


Fig. 2. 2-D wavelet transform of noisy "House" image and its multiresolution support ( $T=2\sigma_n$ ).

where  $l =$

|                 |                                  |                                  |                 |
|-----------------|----------------------------------|----------------------------------|-----------------|
| LL <sub>3</sub> | HL <sub>3</sub>                  | HL <sub>2</sub>                  | HL <sup>1</sup> |
| LH <sub>3</sub> | H <sub>3</sub><br>H <sup>3</sup> |                                  |                 |
| LH <sup>2</sup> |                                  | H <sub>2</sub><br>H <sup>2</sup> |                 |
| LH <sup>1</sup> |                                  |                                  | HH <sup>1</sup> |

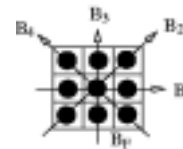


Fig. 3. 4 directional structuring elements each with a size of  $1 \times 3$ .

falsely detected by the noise with the preservation of the spatial clustering of significant coefficients by the edges. Based on this observation, new methods for wavelet shrinkage combined with morphological clustering filter are proposed as follows:

#### Method 1

- (1) Compute the wavelet decomposition of the noisy image.
- (2) By hard thresholding with threshold  $T_1$ ,  $S^l(\underline{n})$  is obtained.
- (3) Apply the MCF on  $S^l(\underline{n})$ :

$$\tilde{S}^l(\underline{n}) = \left\{ \max_{i \in \{1, \dots, M\}} \left[ (S^l \ominus B_i)(\underline{n}) \right] \right\} \oplus B_F(\underline{n}).$$

- (4) Manipulate the wavelet coefficient by  $w_l^{new}(\underline{n}) = \tilde{S}^l(\underline{n})w_l(\underline{n})$ .
- (5) Reconstruct the image by inverse wavelet transform.

When step 3 is omitted, method 1 becomes the hard thresholding technique used in [3, 4].

#### Method 2

- (1) Compute the wavelet decomposition of the noisy

image. (2) By hard thresholding with threshold  $T_{21}$ ,  $S^l(\underline{n})$  is obtained. (3) Apply the MCF on  $S^l(\underline{n})$ :

$$\tilde{S}^l(\underline{n}) = \left\{ \max_{i \in \{1, \dots, M\}} \left[ \left( S^l \ominus B_i \right) (\underline{n}) \right] \right\} \oplus B_F(\underline{n}).$$

(4) Manipulate the wavelet coefficient by  $w_l^{new}(\underline{n}) = \tilde{S}^l(\underline{n}) w_l(\underline{n})$ . (5) Re-apply soft thresholding with threshold  $T_{22} (< T_{21})$  on  $w_l^{new}(\underline{n})$ . (6) Reconstruct the image by inverse wavelet transform.

Note that the soft thresholding used in wavelet shrinkage [2] is given by

$$N_s(w, T) = \text{sgn}(w) (|w| - T)_+,$$

where  $(x)_+$  takes the value  $x$  for positive  $x$  and zero otherwise.

When step 5 is omitted, method 2 is equivalent to method 1. As can be seen, these new methods can be easily implemented by inserting morphological clustering filtering into the wavelet shrinkage algorithm.

#### 4. SIMULATION RESULTS

The performance of new methods is evaluated by signal-to-noise ratio (SNR) gain. The SNR gain is given by

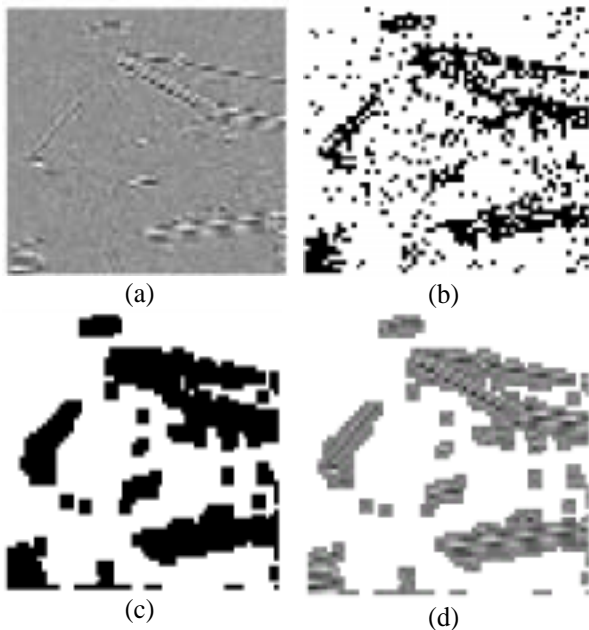


Fig. 4. MCF applied on  $S^{LH2}$ : (a) LH2, (b)  $S^{LH2}$ , (c) MCF output, (d) edge area.

$$\begin{aligned} SNR_{gain} &= SNR_{output} - SNR_{input} \\ &= 10 \cdot \log_{10} \frac{\sigma_s^2}{\sigma_r^2} - 10 \cdot \log_{10} \frac{\sigma_s^2}{\sigma_n^2} \\ &= 10 \cdot \log_{10} \frac{\sigma_n^2}{\sigma_r^2}, \end{aligned} \quad (3)$$

where  $\sigma_n^2$  is the variance of the additive white Gaussian noise,  $\sigma_s^2$  is the variance of the original signal and  $\sigma_r^2$  is the variance of the remaining noise, i.e., the variance of error between the original and the reconstructed signal. Since the threshold value is known to be related to noise variance, in this simulation, the thresholds are set to  $T = T_{12} = T_{21} = 2\sigma_n$  and  $T_{22} = \sigma_n / 2$  for performance comparison. The value  $\sigma_n$  is directly obtained from input noise. And Daubechies wavelet  $D_3$  [8] is used.

Table 1 shows the gain in SNR obtained with denoising methods for varying input SNR of given noisy ‘‘House’’ and ‘‘Pepper’’ images. Clearly, new methods combined with the morphological clustering filter outperform all other methods (hard and soft thresholding). It is concluded that the noise suppression performance of thresholding-based de-noising methods in the wavelet domain can be increased using the morphological clustering filter. The restored images by new and other methods are shown in Figs. 5 and 6. The images restored by new methods clearly are less noisy than those obtained by hard and soft thresholding methods. It is observed that the restored images (see Fig. 5 (e)) contain spurious cross-like features especially around the edges. These features are due to unsuppressed noisy wavelet coefficients in the high level [6]. Since the morphological clustering filter with the same size of structuring element is applied on all multiresolution supports  $S^l$  and a single coefficient in level  $l$ , corresponds to 4 coefficients in level  $l+1$ , the location of a significant coefficient in the higher level is greatly expanded compared to the lower level. Thus, there is a possibility that the significant coefficients detected in the higher level contain more noise components. Therefore, to reduce spurious cross-like features, the morphological clustering filter having a small sized structuring element in the higher level might be needed.

#### 5. CONCLUSIONS

In this paper, the morphological clustering filtering techniques applied to wavelet shrinkage are presented. It is shown that a simple morphological clustering filter enables us to separate the significant wavelet coefficients corresponding to the image component from those corresponding to the noise. The simulation results indicate that noise suppression performance of wavelet shrinkage can be increased using the proposed morphological filter.

Table 1. Comparative de-noising results.

| “House” image | Hard Thresh old | Soft Thresh old | Proposed Method1 | Proposed Method2 |
|---------------|-----------------|-----------------|------------------|------------------|
| SNRinput (dB) | SNR gain (dB)   |                 |                  |                  |
| 0             | 4.77            | 9.71            | 10.34            | 10.81            |
| 5             | 4.11            | 7.21            | 8.17             | 8.50             |
| 10            | 3.28            | 4.87            | 6.00             | 6.37             |
| 15            | 2.43            | 2.62            | 3.96             | 4.25             |
| 20            | 1.20            | 0.47            | 2.02             | 2.28             |

| “Pepper” image | Hard Thresh old | Soft Thresh old | Proposed Method1 | Proposed Method2 |
|----------------|-----------------|-----------------|------------------|------------------|
| SNRinput (dB)  | SNR gain (dB)   |                 |                  |                  |
| 0              | 4.47            | 9.04            | 9.08             | 9.46             |
| 5              | 3.81            | 6.36            | 6.77             | 7.08             |
| 10             | 2.86            | 3.86            | 4.59             | 4.93             |
| 15             | 1.80            | 1.58            | 2.60             | 2.86             |
| 20             | 0.52            | -0.61           | 0.78             | 1.04             |

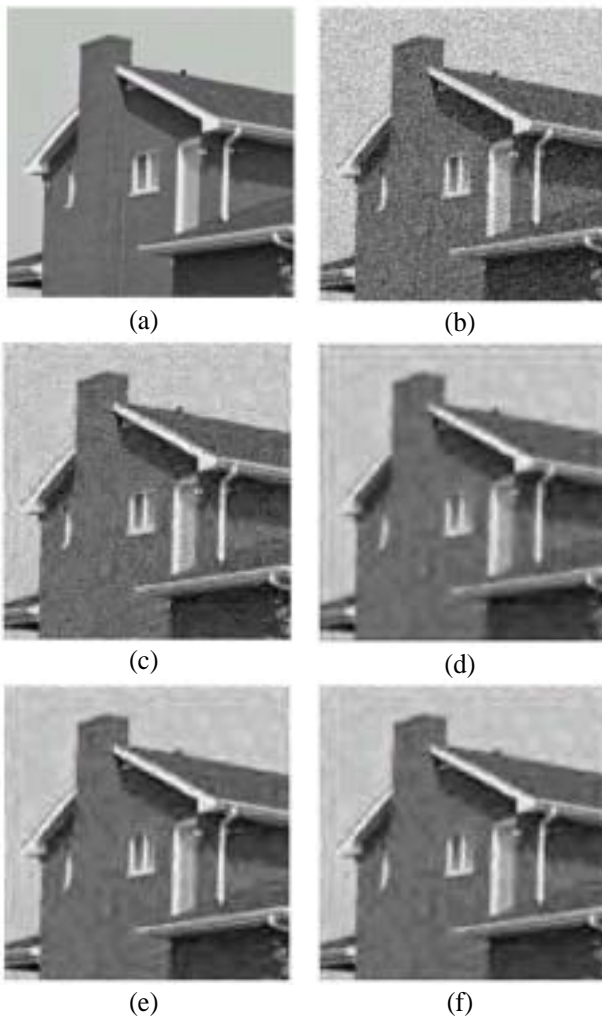


Fig. 5. Restored “House” images: (a) Original image, (b) Noisy image (SNR input=5 dB), (c) Hard threshold, (d) Soft threshold, (e) Method 1, (f) Method 2.

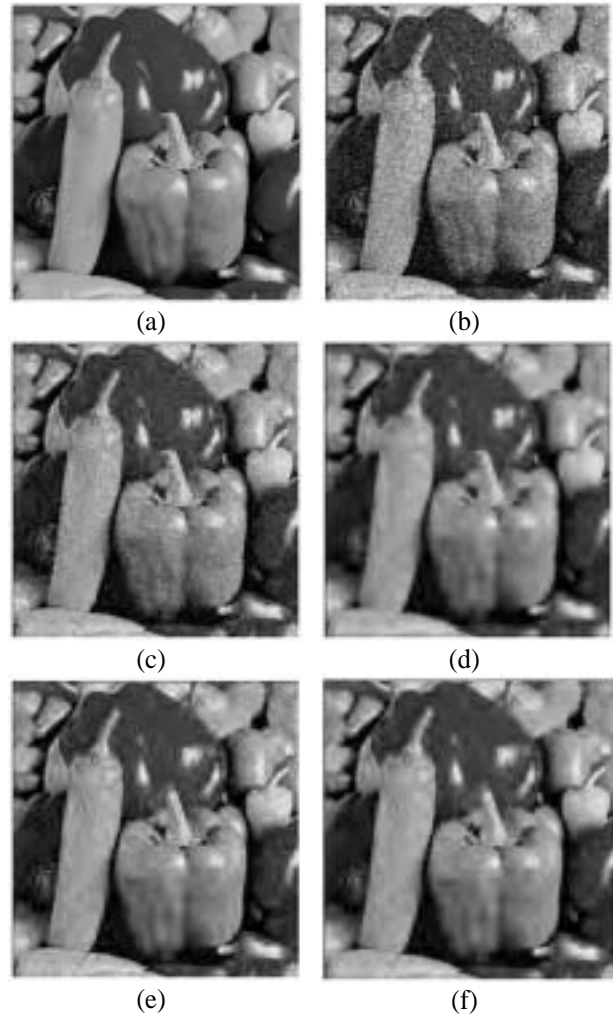


Fig. 6. Restored “Pepper” images: (a) Original image, (b) Noisy image (SNR input=5 dB), (c) Hard threshold, (d) Soft threshold, (e) Method 1, (f) Method 2.

**REFERENCES**

- [1] G. Strang and T. Nguyen, *Wavelets and Filter banks*, Wellesley-Cambridge Press, 1997.
- [2] D. L. Donoho, “De-noising by soft thresholding,” *IEEE Trans. Inform. Theory*, vol. 41, pp. 613-627, 1995.
- [3] J.-L. Starck and F. Murtagh, “Multiresolution support applied to image filtering and restoration,” *Graphic Models and Image Process.*, vol. 57, no. 5, pp. 420-431, 1995.
- [4] N. Weyrich and G. T. Warhola, “Wavelet shrinkage and generalized cross validation for image de-noising,” *IEEE Trans. Image Process.*, vol. 7,

- no. 1, pp. 82-90, January 1998.
- [5] Y. Xu, J. B. Weaver, Jr. D. M. Healy, and J. Lu, "Wavelet transform domain filters: a spatially selective noise filtration technique," *IEEE Trans. Image Process.*, vol. 3, no. 6, pp. 747-758, November 1994.
- [6] M. Malfait and D. Roose, "Wavelet-based image de-noising using a Markov random field a priori model," *IEEE Trans. Image Process.*, vol. 6, no. 4, pp. 549-565, April 1997.
- [7] G. Mallat, "Zero-crossings of a wavelet transform," *IEEE Trans. Inform. Theory*, vol. 37, pp. 1019-1033, July 1991.
- [8] Daubechies, "Orthonormal bases of compactly supported wavelets," *Comm. on Pure and Applied Math.*, vol. 41, pp. 909-996, 1988.
- [9] K. W. Chan and K. L. Chan, "Subband VPIC with classified joint vector quantization," *Signal Proc.: Image Comm.*, vol. 13, pp. 154-153, April 1998.
- [10] J. Luo, C. W. Chen, K. J. Parker, and T. S. Huang, "A scene adaptive and signal adaptive quantization for subband image and video compression using wavelets," *IEEE Trans. Circuits System Video Tech.*, vol. 7, no. 2, pp. 343-357, April 1997.
- [11] K. Ramchandran and M. T. Orchard, "An investigation of wavelet-based image coding using an entropy-constrained quantization framework," *IEEE Trans. Signal Process.*, vol. 46, no. 2, pp. 342-353, February 1998.
- [12] M. Hong, J. Oh, and S.-H. Park, "Improved alternative sequential filter-edge detector," *IEICE Trans. Fundamentals*, vol. E84-A, no. 5, pp. 1352-1356, May 2001.



**Jinsung Oh** received his B.S. and M.S. degrees in Electrical Engineering from Yonsei University, Korea in 1987, and 1989, respectively, and his Ph.D. degree in Electrical Engineering from the University of Pittsburgh, U.S.A. in 1998. He is currently an Assistant Professor in the School of Electrical Engineering at Halla Uni-

versity, Korea. His research interests include image processing, architecture, and algorithms for multimedia systems.



**Heesoo Hwang** received his B.S., M.S. and Ph.D. degrees in Electrical Engineering from Yonsei University in 1986, 1988, and 1993, respectively. From 1993 to 2000, he worked in system engineering for the Korea High-Speed Rail Development project as a senior and a principal researcher in KRRI and KHSR, respectively.

Since 2001, he is an Assistant Professor in the School of Electrical Engineering at Halla University. His research interests include pattern classification, event prediction, and surveillance using fuzzy logic, neural network, and evolutionary algorithms.



**Changhoon Lee** was born in Seoul. He received his B.S., M.S., and Ph.D. degrees in Electrical Engineering from Yonsei University in 1983, 1985, and 1991, respectively. From 1991-1996, he worked as a senior research engineer at LG Industrial Systems. Currently, he is a

Professor in the School of Electrical Engineering at Halla University. His interests include factory automation, control techniques, and machine vision system.



**Younam Kim** received his B.S. in Electrical Engineering from Busan National University, Busan, Korea, in 1981, and M.S. and Ph.D. degrees in Electrical Engineering from Yonsei University, Seoul, Korea in 1983 and 1989, respectively. From 1984-1988 he worked as a junior research engineer at L.D., and Samsung Elec-

tronic Technology Research Institute, and from 1989-1995, he worked as Chief Research Engineer at the SSangyong Motors Technology Research Institute. Currently he is a Professor in the Department of Electrical Engineering at Halla University.